A Multi-body Approach to Aircraft Dynamic Ground Loads Computation

Vikram Sohoni Ph.D*, Frode Engelsen Ph.D**, Jinzhong Wang Ph.D*
*MSC.Software Corp., **The Boeing Company

Keywords: *multi-body, aeroelasticity, trim, aircraft, dynamics*

Abstract

Dynamic ground loads on aircraft components due to maneuvers such as landing and taxi maneuvers are traditionally computed using finite element or proprietary dynamics codes. Limitations inherent in these approaches make simulation of such maneuvers with varying aircraft conditions tedious and error prone. A general purpose multi-body dynamics based approach provides a platform for seamless integration of multi-disciplinary aircraft sub-systems including airframe aeroelasticity, articulated landing gear, high fidelity tire modeling, landing gear oleo and sliding contacts, flight control system amongst others into one model. This paper presents one such multi-body modeling approach for computation of dynamic ground loads and by extension component stresses and strains.

1 Introduction

The computational system presented in this paper automatically assembles governing equations multi-disciplinary systems. Mass bearing components are interconnected with internal forces or kinematic constraints. Flexible components are represented using a modal formulation. Dynamical components such as controls systems are incorporated by including component appropriate modeling equations in the governing equations. These governing equations are adapted to compute trim aircraft model for specified operating conditions such as fuel load, airspeed, sink speed, load factors etc. Dynamic analysis starting from trimmed initial conditions is performed using numerical integration methods. This formulation allows for models to undergo larger translational and rotational displacements with superimposed small deformations of flexible components. MSC.Software's SimXpert product[1] embodies this modeling methodology. This paper is organized in the following manner. Technical assets available in the modeling and simulation system are presented in sections 2 through 8. These include modeling of interconnected flexible bodies. Modeling effects such as tire and ground interaction and sliding contact between landing gear components are presented next. This is followed by analysis methods to compute trim and perform dynamic analysis from this trim condition thereafter. Use of these assets for dynamic ground loads analysis is demonstrated with a design study of a landing maneuver. This design study investigates the effect load factor on wing root loads during the landing maneuver.

2 Multi-body formulation

2.1 Introduction

Multi-body systems are modeled as connected system of rigid and flexible bodies. Bodies may be connected to one another by kinematic constraints or forces. Rigid bodies are modeled with 6 degrees of freedom (3 translational and 3 rotational). The rigid bodies can undergo large translation and rotational displacements. Global location of a point on the rigid body is given as:

$$r_p^G = R_i + A^{iG}\ r_p^i \qquad (1)$$

where:

R_i = position vector of a rigid body i in space
r_p^i = position vector of point p in local body frame for body i

r_p^G= position vector of point p in the global reference frame
A^{iG}= transformation matrix from the part i local frame to global frame
Flexible bodies are modeled with 6 rigid body degrees of freedom and assumed modes for linear elastic deformation super imposed on the large rigid body displacement.

Flexible components such as the airframe are represented by a modal superposition method.

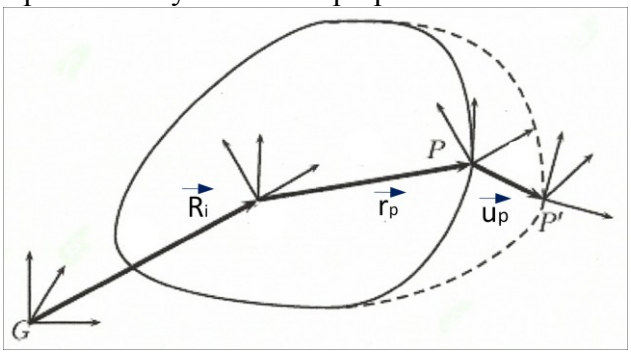

Figure 1 Deformation of Node on Flexible Body

Extending equation 1 to a flexible body as shown in figure 1, displacement of a node *P* on a flexible body is given as

$$r_p^G = R_i + A^{iG}\left(r_p^i + \sum_{j=1}^{n} \phi_j q_{f_j}\right) \quad (2)$$

where

n= number of modes
ϕ=mode shape
q_f=flexible generalized coordinates; a sub-set of the model generalized coordinates, q

2.2. Equations of motion

Generic equations of motion for a flexible body are represented as [3]:

$$[M]\{\ddot{q}\} + [K]\{q\} + [C]\{\dot{q}\} = \{f(q, \dot{q}, \ddot{q})\} \quad (3)$$

where

[M] = mass matrix
[K] = stiffness matrix
[C] = damping matrix
$\{q\}$ = generalized coordinates. This includes rigid body and flexible coordinates.
$\{f(q, \dot{q}, \ddot{q})\}$ = applied forces.

2.3 Kinematic connections between bodies

Rigid and Flexible bodies can be connected by a wide variety of kinematic constraints. These constraints allow for modeling of any combination of rotation and translational articulation between connected rigid and flexible bodies.

2.4 Applied forces

Applied forces include single and vector point forces. Modal forces are applied on rigid body and flexible modes of a flexible body. Modal forces are of several different types including superposition of stored modal loads.

3 Aerodynamic modeling

The applied modal forces accommodate modeling of unsteady or quasi-steady aerodynamics. The aerodynamic forces can be determined using the lifting line theory, doublet lattice method or other methods. Doublet lattice aerodynamics are calculated in the frequency domain, but converted to a time domain form using a rational function approximation. The user will have a choice between a quasi-steady or unsteady aerodynamic formulation.

3.1 Quasi-steady Aerodynamics

The quasi-steady aerodynamic formulation introduces additional matrix terms in the equations of motion coupling the generalized degrees of freedom.

$$\{P_{aero}(t)\} = p_{dyn}\left([A_0]\{q(t)\} + \frac{1}{V}[A_1]\{\dot{q}(t)\} + [A_\delta]\{\delta(t)\}\right) \quad (4)$$

where

$\{P_{aero}(t)\}$ = Aerodynamic force vector
$p_{dyn} = \frac{1}{2}\rho V^2$ = Dynamic pressure
V =Air speed
ρ =Density of atmosphere
$\{\delta(t)\}$ = Controller states
$[A_0]$ = Generalized aerodynamic stiffness matrix per unit p_{dyn}
$[A_1]$ = Generalized aerodynamic damping matrix per unit p_{dyn}, proportional to generalized coordinate velocity

$[A_\delta]$ = Generalized aerodynamic force matrix per unit p_{dyn}, due to controller application

This computation is implemented as user supplied code that extends the functionality of SimXpert simulation system. Quantities to the right hand side of equation 4 are passed into the user code which returns the aerodynamics forces and moments. Note that dynamic pressure varies with time as the airframe maneuvers in space.

The quasi-steady aerodynamics are calculated from the frequency dependent, oscillatory aerodynamics [*Q(k)*] under the assumption that the real portion is independent of frequency and imaginary portion is proportional to frequency [3].

$$[Q_{quasi-steady}(k)] = [Q(k=0)] + i\frac{k}{k_{small}} Im[Q(k=k_{small})] \quad (5)$$

where

$i = \sqrt{-1}$

k = reduced frequency=$\frac{\varpi b}{V}$

ϖ = angular frequency

b = reference length for the reduced frequency

With these assumptions, the aerodynamic stiffness and damping matrices are calculated as:

$$[A_0] = [Q(k=0)]$$

$$[A_1] = \frac{b}{k_{small}} Im[Q(k=k_{small})]$$

3.2 Unsteady Aerodynamics

With unsteady aerodynamics, additional matrix terms are added (compared to the quasi-steady aero) and additional lag states are introduced as generalized coordinates. The unsteady aerodynamic formulation increases accuracy, but also the computational cost.

The unsteady aerodynamic forces are calculated from the oscillatory aerodynamics based on the well known Roger rational function approximation [4].

4 Tire Ground interaction

4.1 Tire force modeling

Tire forces as function of longitudinal and lateral slips are included in the model as applied forces. The tire model uses the point-follower model for a single contact point with the road profile [2].

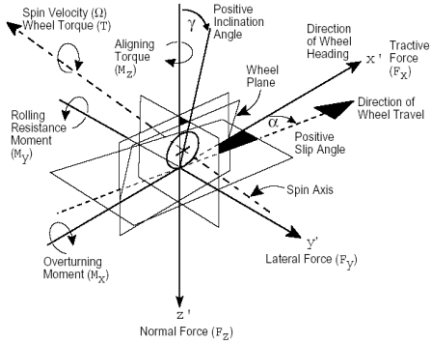

Figure 2 Tire Kinematics and forces

The contact point is the point nearest to the wheel center that lies on the line formed by the intersection of the tire (wheel) plane with the local road plane.

The contact force computed by the point-follower contact method is normal to the road plane. Therefore, in a simulation of a tire hitting a pothole, the point-follower contact method does not generate the expected longitudinal force. In general, the point-follower method is valid for rather smooth roads (road obstacle wavelengths > tire circumference) only.

The more complex equivalent-volume method determines an equivalent contact point and vertical deflection from the volume of intersection of the tire carcass with the road. The equivalent-volume method assumes the tire carcass is a cylinder. Triangular facets describe the road surface.

The normal force of a road on a tire at the contact patch in the SAE coordinates (+Z downward) is always negative (directed upward). The normal force is:

$$F_z = \min\left(0, (F_{zk} + F_{zc})\right) + \min(0, F_{zrim}) \quad (6)$$

where

F_{zk} = normal force due to the tire radial stiffness curve

F_{zc} = normal force due to the tire radial damping

F_{zrim} = normal force due to the tire radial bottoming

The tire forces may be determined by a stiffness and damping coefficient and effective penetration. Alternatively, the tire force and damping characteristics can be supplied in a tabular form.

4.2 Ground/runway definition

Ground definition can be assembled from a set of predefined ground features such as, flat surfaces and obstacles. Continuous obstacles such as sinusoid can be combined with discrete obstacles such as planks, holes etc. to create any desired ground description. Soft soil runways are modeled using an elastic-plastic model. These combinations of features permit modeling of a wide variety of prepared and un-prepared runways.

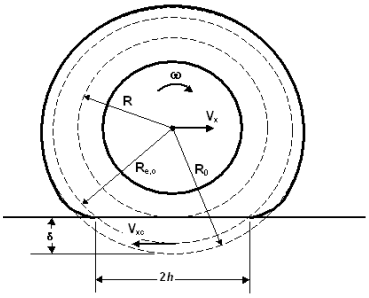

Figure 3 Rolling characteristics of a Tire

5 Landing Gear Strut modeling

Contact between the inner and the outer tubes of the landing gears are modeled using a discrete flexible contact modeling methodology. A bearing at the top of the inner tube applies contact forces on the outer tube at discrete stations along the length of the outer tube. As the bearing slides along the length of the outer tube contact forces are proportionally distributed between the two stations bracketing the bearing location. Similarly, contact between the bearing located at the bottom of the outer tube and the inner tube is modeled. This modeling methodology allows for a smooth application of bearing forces as the inner and outer tube slide relatively to one another during dynamic maneuvers.

6 Controls modeling

Controls modeling equations are included in the governing equations in either the continuous or discrete form.

The continuous controls are represented in the form:

$$\dot{x} = F(x, u, t) \qquad (7)$$
$$y = G(x, u, t)$$

where

x=continuous control states
u=inputs to control system
y= outputs from the control system

Discrete controls are represented in the form:

$$x_{n+1} = h(x_n, u_n, t_n) \qquad (8)$$
$$y_{n+1} = g(x_n, u_n, t_n)$$

where subscripts denote the discrete form of the respective variable.

7 Governing System Equation

Instances of modeling object types described in sections 2 to 6 are assembled into a general multi-disciplinary system. In general, the system of coupled equations is represented as

$$G(y, \dot{y}, t) = 0 \qquad (9)$$

where
y=all solution variables in the system of equations

Variations of these governing equations are adapted for us for different analysis methods.

8 Analysis Methods

8.1 Trim analysis

Trim analysis determines initial conditions for a dynamic analysis [5][6]. This analysis computes the dynamic equilibrium configuration of the aircraft for specified conditions such as sink speed, air speed, load factor, wind velocity, desired airframe attitude etc. At trim the aircraft is in dynamic equilibrium, starting dynamic analysis from this configuration the model will have no transients other than specified velocities and accelerations.

For trim analysis, a subset of the governing equations is assembled into a system of algebraic equations.

Rearranging the governing equation (3) in the following form gives an algebraic systems of equations that is to be solved for the trim conditions

$$[K]q_t - \{f(q_t, \dot{q}_p, \ddot{q}_p)\} = \{-[M]\{\ddot{q}_p\} - [C]\{\dot{q}_p\}\} \quad (10)$$

where

$\dot{q}_p$, $\ddot{q}_p$ = prescribed model velocities and accelerations for trim solution
q_t = compute aircraft states at trim

Equation 10 is a non-linear system of algebraic equations with prescribed right hand side. This system of equations is solved using a Newton-Raphson iterative algorithm. The trim solution requirement of prescribing some model states is enforced by the constraint

$$[B]\{q_t\} = \{q_p\} \quad (11)$$

where

q_p= prescribed sub set of model states
$[B]$=A diagonal Boolean matrix
A value of one on the diagonal of this matrix indicates that the model state of the corresponding row or column is specified. Conversely, a value of zero indicates the corresponding state is to be computed by the solution procedure.

Equation (11) is enforced on trim systems equations by introducing an unknown multiplier such that the system of equations to be solved for trim conditions is

$$[K]q_t - \{f(q_t, \dot{q}_p, \ddot{q}_p)\} = \{-[M]\{\ddot{q}_p\} - [C]\{\dot{q}_p\}\} + [B]^T\{\eta\}$$
$$[B]\{q_t\} = \{q_p\} \quad (12)$$

Equation 12 is a coupled algebraic system of equations to be iteratively solved for during trim solution. Convergence criteria for the trim solution require $\{\eta\} = \{0\}$. This condition guarantees that the model states are trimmed to be consistent with prescribed model state, velocities and accelerations.
Trim constraints as specified in equation 11 are maneuver specific type. Constraints for a pitch trim maneuver where the aircraft is being trimmed to compute the pitch angle given air speed and sink rate are different from those for a taxi maneuver.

8.2 Dynamic Analysis

Time domain numerical integration simulates the maneuver using the trim solution as initial conditions. Several numerical integration methods, such as Gear stiff, HHT (Hilber-Hughes-Taylor), Newmark amongst others, are available for dynamic analysis. These variable step methods change integration step size to maintain integration error accuracy. Variable order methods in this suite also vary integration order in addition to step to maintain accuracy within specified integration error tolerance.

9 Example

9.1 Model description

Application of the methodology presented in sections 2 to 8 is demonstrated using a general aviation model. The airframe shown in figure 4 is modeled with 36 flexible modes in the frequency range of 7.1 to 95 Hz. Aerodynamics are modeling using the methodology described in section 3.

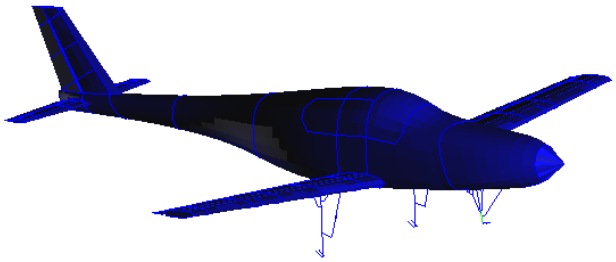

Figure 4 Airframe Structure

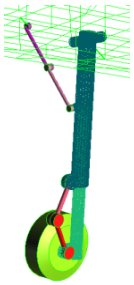

Figure 5 Landing Gear mechanism

The main and nose landing gears are modeled as flexible inner tube sliding inside an outer tube. Contact between the tubes is modeled as described in section 5. Rotational orientation between the tubes is enforced by two scissor links. The outer tube is connected to the wing by a kinematic connection. This kinematic connection allows for the main gear to be stowed in the wing if required for the maneuver. A similar modeling methodology is employed for the nose gear. The inner and outer tubes are represented by 30 flexible and rigid body modes each.
Due to the possibility of tail strike on the runway, contact between the airframe and the runway is modeled. This aircraft model includes two controls; elevator and thrust. The simulation maneuvers are for a symmetric landing.

9.2 Maneuver specification

The maneuver is specified as a landing simulation starting from a pitch trimmed initial condition. Trim conditions are:

Airspeed = 2200 inches/sec
Trim sink speed = 120 inches/sec

A design study is to be performed varying the load factor from 0.5 to 1.5 in 7 steps. Purpose of the design study is to determine peak loads for the specified operating conditions.

For each load factor the aircraft model is to be trimmed for pitch. The trim procedure computes the pitch angle, thrust and elevator deflection for the specified conditions. Simultaneously the solution process loads the airframe with aerodynamic forces to sustain the specified trim flight conditions. Following trim a dynamic analysis is performed for a sufficient duration for the landing event to complete and resulting in capture of the peak landing loads.

Figure 6 shows an animation frame for the aircraft in trimmed flight on approach to the runway. As is evident from the fringe display the maximum structural deformation is at the wing tips.

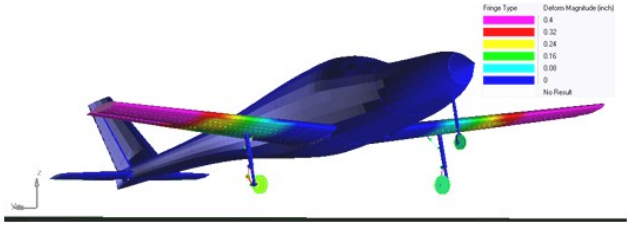

Figure 6 Trimmed flight landing approach

9.3 Results review

Figure 7 shows the airframe pitch angle as a function of time. The simulation starts with the aircraft in trimmed flight followed by a touchdown event and then the aircraft settling on the runway. For load factors in the range 1.16 to 0.5 there is smooth change in the pitch angle as the aircraft goes through these phases of the landing maneuver. For load factors 1.5 and 1.33, however, there is a relatively shape transition in the pitch angle during the touchdown event. This is due to the relatively high aircraft pitch angle for these load factors that causes the tail to strike the runway before the main landing gear hits the runway

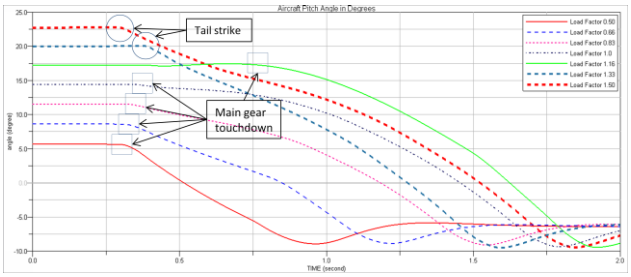

Figure 7 Aircraft Pitch Angle

This is further evidenced by examining the wing root pitch moment in figure 8. For these two simulations there are positive moment spikes in the chart in contrast to absence of such spikes for simulations for load factors 0.5 and 0.66.

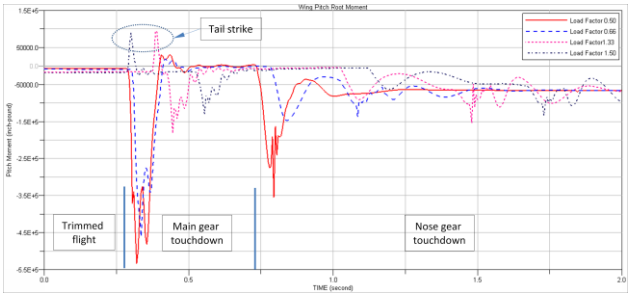

Figure 8 Wing Root Pitch Moment

Chart in figure 9 shows root vertical force as a function of time for the seven simulations. Figure 10 shows the root bending moment for the same simulations.

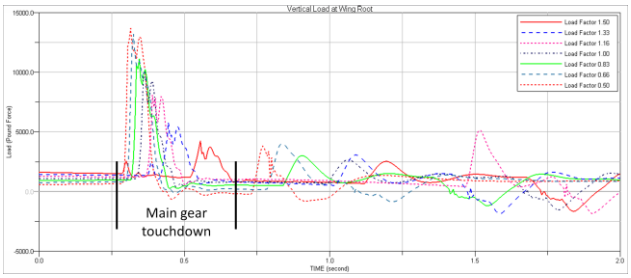

Figure 9 Vertical loads at Wing root

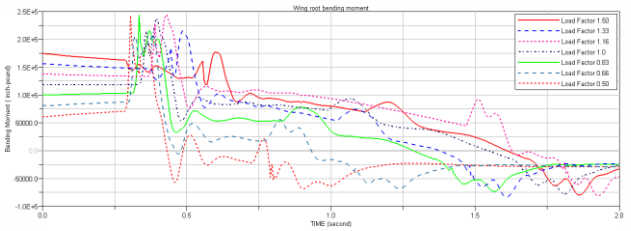

Figure 10 Wing Root bending moment

Figure 11 shows an animation frame for the simulation at a load factor of 1.5 at the instant the tail strike occurs. Areas of highest deformation are in magenta. Large structural deformation is now seen in the area of the tail section of the airframe. This is in contrast to the trimmed flight were deformations in this section were relatively small.

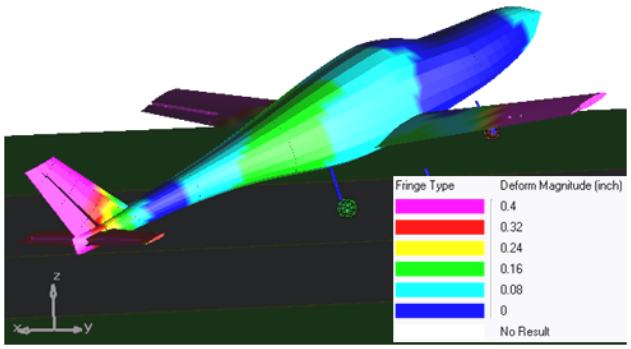

Figure 11 Airframe deformation fringe display for tail strike during landing for load factor 1.5

10 Conclusion

This paper demonstrates the integration of multiple disciplines into a multi-body model. Multi-body modeling methodology provides an effective platform for integrating structure, aerodynamics, ground to tire forces, and controls to name a few. This modeling methodology enables ground load computation for a wide variety of operating conditions and maneuver types.

11 Acknowledgements

The authors would like to acknowledge contributions of their colleagues Doug Hargett, Michael Collingridge, Jim McConville and Doug Neill of MSC.Software and Daniel Rivera, Shih-Chin Wu and Rich Jacobs of The Boeing Company.

References

[1] Hargett D, Sohoni V, McConville J and Kamber P. A Comprehensive Systems Approach for Aircraft modeling., *Proc IFASD 2009*, Seattle, WA, USA, IFASD 2009-057

[2] Adams Software Documentation, MSC Software Corp

[3] Handbook for Aeroelastic Analysis, MSC/NASTRAN Version 65, The MacNeal-Schwendler Corporation, Los Angeles, CA, 1987.

[4] Roger K. Airplane Math Modeling Methods for Active Control Design, Structural Aspects of Active Controls, AGARD CP-228, Aug. 1977, pp. 4-11.

[5] Shearer C and Cesnik C. Nonlinear Flight Dynamics of very flexible Aircraft, *J. of Aircraft*, vol.44, No. 5, pp. 1528-1545, 2007

[6] Baldelli D, Chen P and Panza J. Unified Aeroelastic and Flight Dynamics Formulation via Rational Function Approximation. *Journal of Aircraft*, vol. 43, No. 3, pp.763-772, 2006

12 Contact Author Email Address

The contact author email address Vikram Sohoni.

vikram.sohoni@mscsoftware.com

Copyright Statement